

Hadron spectroscopy and interactions

Jeremy R. Green*

*John von Neumann-Institut für Computing NIC, Deutsches Elektronen-Synchrotron DESY,
Platanenallee 6, 15738 Zeuthen, Germany*

E-mail: jeremy.green@desy.de

In recent years, lattice QCD calculations of hadron spectroscopy have concentrated on resonances and shallow bound states detected via poles in two- and three-hadron scattering amplitudes. Hadron interactions have therefore become a key focus. In these proceedings, I review the current state of the art and recent advances in methods for studying hadron interactions via finite-volume spectroscopy and finite-volume quantization conditions. I will also review recent spectroscopy studies and results presented at Lattice 2025, with a focus on charmed mesons, the doubly charmed tetraquark, and the doubly bottom tetraquark.

*The 42nd International Symposium on Lattice Field Theory (LATTICE2025)
2-8 November 2025
Tata Institute of Fundamental Research, Mumbai, India*

*Speaker

1. Introduction

The goal of hadron spectroscopy is understanding the composite states formed from quarks and gluons. In the last decade, the focus of these studies on the lattice has shifted from hadrons that are stable in QCD to those that are unstable, decaying to other hadrons. Formally, both stable and unstable states exist as poles in the partial wave scattering amplitudes of the stable hadrons to which they couple; see Fig. 1. It is thus necessary to study scattering states in order to investigate resonance and virtual-state poles.

Experimental studies of the hadron spectrum are still very active, in part because of the many exotic hadrons that have been discovered. In the broadest sense, these are states not predicted by the standard quark model in which mesons are quark-antiquark states and baryons are three-quark states. Beyond simple disagreements with the precise quark model predictions, this also includes states that contain four or more quarks and mesons with J^{PC} not allowed by the quark model.

In addition to the considerable interest in exotic hadrons, lattice QCD calculations are also being used to study conventional unstable hadrons, including the lightest ones such as $f_0(500)$, $\rho(770)$, and $\Delta(1232)$. Multihadron physics is interesting in its own right: for instance, two or three pions can appear as intermediate states in the hadronic vacuum polarization or as final states in kaon decay. Finally, the techniques of hadron spectroscopy can be used to better isolate states for hadron structure studies, as discussed in the plenary talk by Barca [1].

This review is divided into two parts. Section 2 reviews methods for hadron spectroscopy and recent developments. Some specific hadron systems that have been investigated in the literature and at this conference are discussed in Section 3. An outlook is given in Section 4.

2. Methods

The standard approach for studying scattering amplitudes (and stable hadrons) is finite-volume spectroscopy. This can be organized into four main steps:

1. Computing matrices of two-point correlation functions,

$$C_{ij}(t) \equiv \langle O_i(t) O_j^\dagger(0) \rangle, \quad 1 \leq i, j \leq N_{\text{op}}, \quad (1)$$

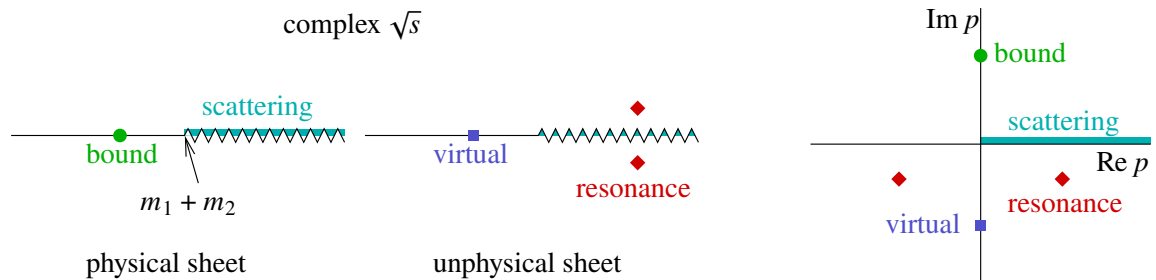


Figure 1: Locations of physical scattering and possible poles for a two-particle partial wave amplitude. Left: on the complex centre-of-mass energy plane, which has physical and unphysical Riemann sheets resulting from a branch cut starting at threshold. Right: on the complex scattering momentum plane, which opens the cut via $\sqrt{s} = \sqrt{m_1^2 + p^2} + \sqrt{m_2^2 + p^2}$.

with the N_{op} interpolating operators O_i chosen to have definite flavour, momentum, and rotational quantum numbers.

2. Estimating the low-lying finite-volume energies E_n from the time dependence of $C_{ij}(t)$.
3. Applying finite-volume quantization conditions to constrain models of partial wave scattering amplitudes using the finite-volume energies.
4. Analytically continuing the amplitudes to find poles corresponding to hadrons (bound states, virtual states, or resonances).

For each of these steps, the state of the art and recent developments will be discussed in a subsection below.

An alternative approach, used less widely, is the HAL QCD method. This requires an analogous series of steps:

1. Computing hadron-hadron correlation functions,

$$F(\mathbf{r}, t) \equiv \int d^3\mathbf{x} \left\langle O_{H_1}(\mathbf{x}, t) O_{H_2}(\mathbf{x} + \mathbf{r}, t) O_{H_1 H_2}^\dagger(0) \right\rangle, \quad (2)$$

where O_{H_i} are local interpolating operators for the two interacting hadrons separated by \mathbf{r} and $O_{H_1 H_2}$ is an interpolating operator for the two-hadron system.

2. Estimating the nonlocal interaction potential $U(\mathbf{r}, \mathbf{r}')$ from the correlation function. This has a scheme dependence coming from the choice of local interpolating operators and is usually approximated using the leading-order term in a derivative expansion, $U(\mathbf{r}, \mathbf{r}') \approx V^{\text{LO}}(r) \delta^{(3)}(\mathbf{r} - \mathbf{r}')$.
3. Fitting the potential using model functions $V(r)$.
4. Solving the Schrödinger equation using the potential models to determine bound state energies and partial wave amplitudes, which are scheme independent.

As this method is likely to have quite different systematic uncertainties, it provides a valuable alternative to finite-volume spectroscopy. However, the focus of this section is on the standard approach.

2.1 Correlation functions

The simplest and oldest methods for computing correlation functions of interpolating operators built from quark fields are to use (smeared) point sources or Coulomb-gauge wall sources. These can be effective for determining the masses of isolated stable hadrons; however, the restricted spatial structure of the interpolating operators makes a calculation of the full spectrum of scattering states infeasible. These methods are also sometimes associated with asymmetric correlation functions, i.e. with differing source and sink interpolating operators, which can suffer from non-positive-definite correlation functions and non-monotonic behaviour of effective energies. The latter can risk misidentifying even ground-state energies.

One can produce a greater variety of interpolating operators, including nonlocal ones that couple well to scattering states, by combining point sources with sequential- and stochastic-source methods such as in Refs. [2–4].

All-to-all methods allow for more reuse of data and a better cost scaling with the number of interpolating operators. In recent years, position-space sparsening methods have been explored [5, 6]. These are based on replacing the spatial sums used for momentum projection with reduced sums over regular grids or random subsets of the lattice. If the subsets are sufficiently small, it is feasible to compute and save the all-to-all (smeared) quark propagator between points belonging to the subsets. Since smearing has a physically large footprint, a substantial sparsening is possible with negligible loss of signal quality.

The most widely used all-to-all method is *distillation* [7, 8], which is based on computing the all-to-all propagator within a subspace of dimension $4N_{\text{LapH}}$ on each timeslice. This “distillation subspace” is formed from the lowest N_{LapH} eigenmodes of the three-dimensional Laplacian, and the corresponding Laplacian-Heaviside (LapH) smearing of quark fields is a projection onto this subspace. In recent years, some variants and improvements have been explored. One avenue is improving the smearing using *quark distillation profiles*, which allow for a more optimal tuning within the distillation space [9]; an update combining this with covariant derivatives was presented by Urrea-Niño [10, 11]. Going in a different direction, the distillation subspace can be varied: one option is to use plane waves in Coulomb gauge [12]. The latter was used in a study of the nuclear spin-orbit force within the HAL QCD method, presented by Sugiura [13].

One of the drawbacks of distillation is the high cost of contractions for local interpolating operators with four or more quarks at the same point, which scales as N_{LapH}^5 or worse. Two solutions have been developed: the first constructs a localized basis for the distillation space [14] and the second incorporates position-space sparsening [15]. Stump presented an application of the latter to the doubly charmed tetraquark [16].

A universal problem for multihadron correlation functions is the possibly large number of Wick contractions. Naïvely, the cost is factorial in the number of quarks of each flavour; however, many of the intermediate expressions appear repeatedly. Much work has been done to develop algorithms that reduce this cost [17–22]; one method was presented by Chakraborty [23].

For finite-volume multihadron spectroscopy, scaling to large volumes is also very challenging. In distillation, N_{LapH} must be scaled proportionally to the physical three-dimensional volume L^3 to maintain a constant smearing radius. Since multi-meson systems involve only rank-2 tensors in the distillation space, their contraction cost scales as $N_{\text{LapH}}^3 \propto L^9$. Systems with one or two baryons have a cost scaling with $N_{\text{LapH}}^4 \propto L^{12}$ [19, 24]. The density of states is also a problem, since N_{op} should be scaled with the number of states in the energy interval of interest and the naïve contraction cost is proportional to N_{op}^2 . For fixed total momentum and a fixed energy interval, the number of two-hadron states asymptotically scales proportionally to L^3 , which increases to L^6 for three-hadron states. Furthermore, as the gaps between energy levels become smaller, we need higher precision to get useful constraints from finite-volume quantization conditions. Altogether, in the large-volume regime, we get an extremely rapid cost scaling with box size. New ideas may be helpful here.

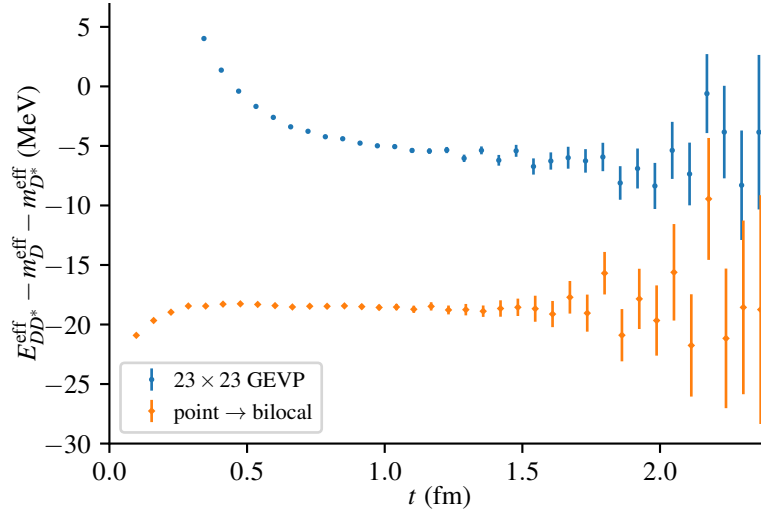


Figure 2: Difference between the ground-state effective energy of a DD^* system and the sum of effective masses of a D and a D^* meson. Blue circles are obtained from solving a GEVP for a symmetric correlator matrix with $N_{\text{op}} = 23$; orange diamonds are obtained from a single asymmetric correlation function with local creation operator and bilocal annihilation operator.

2.2 Lattice spectrum

The starting point for estimating energy levels from a matrix of two-point correlation functions is its spectral decomposition:

$$C_{ij}(t) = \sum_n e^{-E_n t} Z_{in} Z_{jn}^*, \quad Z_{in} \equiv \langle \Omega | \mathcal{O}_i | n \rangle, \quad (3)$$

where thermal effects have been neglected. Having an $N_{\text{op}} \times N_{\text{op}}$ matrix of correlation functions is very important, since it is possible to identify up to N_{op} near-degenerate energy levels via the rank of the matrix that multiplies the exponential.

The standard analysis of a correlator matrix is to solve a generalized eigenvalue problem (GEVP) [25, 26],

$$C(t)v_n(t, t_0) = \lambda_n(t, t_0)C(t_0)v_n(t, t_0). \quad (4)$$

This is a *variational method* in that it implicitly finds an optimal linear combination $\bar{\mathcal{O}}_n = \sum_i (v_n^\dagger)_i \mathcal{O}_i$ for coupling to state n , and $\lambda_n(t, t_0) \approx e^{-E_n(t-t_0)}$. It has been proven [27] that for a particular choice of the reference time t_0 , one gets estimators for the low-lying energy levels with good asymptotic behaviour:

$$-\frac{d}{dt} \log \lambda_n(t, t_0) = E_n + O\left(e^{-(E_{N_{\text{op}}} - E_n)t}\right). \quad (5)$$

By increasing N_{op} , one can obtain a faster convergence to the energies.

Figure 2 illustrates the importance of using a large symmetric correlator matrix and the danger of using a single asymmetric correlator. This particular example of the latter produces a very long and stable plateau, lasting for more than 1 fm with error below 1 MeV. The GEVP produces a completely different, much later and worse looking, plateau. Naïvely looking at this plot, one is tempted to prefer the asymmetric correlator. However, the relevant length scale is the inverse of

the energy gap ΔE governing corrections to the effective energy. For this two-hadron system and a single correlation function, $\Delta E^{-1} \approx 6$ fm, so that a plateau of length 1 fm is inadequate. The GEVP, on the other hand, increases the effective energy gap significantly, shrinking the relevant length scale severalfold. For this reason, one should expect the GEVP plateau to be more accurate, and the asymmetric plateau, disagreeing with it, is probably incorrect. Similar issues have plagued past studies of baryon-baryon systems [28, 29]; see the plenary talk by Nicholson on this topic [30, 31].

In recent years, there have been new efforts to better use the time dependence of correlation functions or matrices to extract information about the spectrum. One strategy is to apply regularized Laplace filters, which suppress correlations and alter the spectral weights [32]. Other methods aim to generalize effective masses and GEVPs to incorporate data from many or all source-sink separations t rather than just a pair of late ones [33–39]: these include the new application of Lanczos-type algorithms to the transfer operator e^{-aH} as well as a revival of older ideas such as the Prony and generalized pencil-of-function methods. In the absence of noise and in suitable limits, these methods are equivalent and yield estimators that converge more rapidly to energy levels. The main difficulties come from having an exact representation of a correlator containing noise, which generally does not have a positive-definite spectral representation. Within this family, Ostmeyer presented a truncated Hankel correlator method, which uses rank- k approximations of a Hankel matrix containing the full correlator data [for a scalar correlator, the matrix is $H_{ij}(t) = C(t + (i + j)a)$] as closed-form alternatives to multi-state fits [38, 40]. With some time having passed since the Lanczos proposal, it is now seeing some applications: Perry presented a study of nucleon-nucleon data using this method including two-sided bounds the method provides for energies [41–43].

2.3 Finite-volume quantization

Quantization conditions provide the relationship between the finite-volume energies that we can compute on the lattice and the infinite-volume scattering amplitudes and bound states that are studied in experiments. For single hadrons or deeply bound states, the relationship is simple: corrections are exponentially suppressed and the finite-volume state is a good approximation to the infinite-volume state. For two-hadron systems, there is now a seemingly mature formalism following years of developments: in addition to dealing with arbitrary coupled channels and arbitrary spin, one can also compute decays, transitions, and matrix elements. A toy-model investigation of the latter for a range of binding energies was presented by Ortega-Gama [44, 45].

Three-particle quantization conditions are increasingly being applied to real data (see Section 3.2), although they are not yet fully general. Sharpe presented quantization conditions for an $N\pi\pi$ system with maximal isospin [46, 47]; see also the plenary talk reviewing three-particle amplitudes by Sharpe [48]. Going beyond three particles, a perturbative study of a finite-volume four-pion system was presented by Mukherjee [49].

Returning to the two-particle case, there have been recent developments despite the maturity of the formalism. These have been instigated by the realization that Lüscher’s quantization conditions break down below threshold in the presence of *left-hand cuts* [24, 50]. Such cuts are shown in Figure 3 and occur due to the exchange of particles in crossed channels (t and u channel). They can lie close to the threshold in cases when two heavy hadrons exchange a light hadron; in particular, this was noted as a problem due to pion exchange in two-baryon and DD^* systems.

By now, five different solutions have been developed. In chronological order:

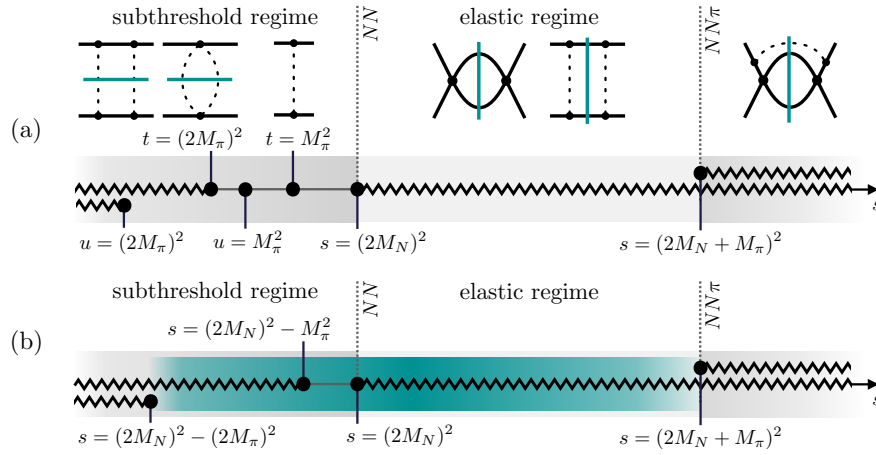


Figure 3: Analytic structure of the NN scattering amplitude: (a) poles and cuts at fixed scattering angle and (b) cuts after partial-wave projection. Standard two-body quantization conditions only deal with the elastic two-particle branch cut. Reproduced from Ref. [51] under the Creative Commons Attribution License (CC-BY-4.0).

1. Using the plane-wave basis to quantize a scattering equation such as a Lippmann-Schwinger equation in finite volume [52, 53]. An application of this was presented by Shrimal [54, 55].
2. Modified Lüscher quantization conditions to obtain a short-distance quantity that is related to the scattering amplitude via integral equations [51, 56].
3. Three-particle quantization, with the two-particle amplitude obtained via LSZ reduction [57, 58]. An application of this was presented by Raposo [59].
4. Modified Lüscher quantization conditions applied to a modified effective range expansion [60, 61].
5. Quantization conditions based on an N/D representation of the amplitude [62].

As discussed in Section 3.4, the three-particle approach is particularly suited to systems such as DD^* , which becomes $DD\pi$ at the physical pion mass where D^* is a resonance, since it works smoothly across the transition from two to three particles.

2.4 Amplitudes and analytic continuation

A commonly-used strategy for describing scattering amplitudes is to fit with a variety of simple analytic models, which can then be trivially continued into the complex plane to find poles. Among the models that yield good descriptions of the lattice spectra, the scatter of results is used to estimate systematic uncertainty.

One way of improving on this approach is to impose stronger physics constraints on the models. In Ref. [63], crossing symmetry of the $\pi\pi$ scattering amplitude (Roy equations) was used to filter out unphysical models, yielding smaller systematic uncertainty on the location of the σ -resonance pole.

An alternative strategy presented by Salg is to avoid explicit analytic models [64, 65]. Instead, the amplitudes are first constrained on the real axis using Bayesian methods similar to Gaussian processes, then continued to the complex plane using Nevanlinna-Pick interpolation.

3. Hadron systems

3.1 Two light mesons

For the simplest resonances involving pions and kaons, lattice calculations are maturing. Refs. [66, 67] presented a study of the $\rho(770)$ and $K^*(892)$ in $\pi\pi$ and πK scattering using one ensemble with physical quark masses; the former was also studied at the physical pion mass by Refs. [68, 69]. We are thus approaching the possibility of precision $\pi\pi$ physics, which calls for an effort to control all sources of systematic uncertainty. Talks at this conference went in different directions: Valois laid the groundwork for $\pi\pi$ scattering with staggered fermions [70], Morandi studied $\pi\pi$ systems using spectral reconstruction techniques valid above the inelastic threshold [71], and Erben presented a study of the rare decay $B \rightarrow K^*(\rightarrow K\pi)\ell^+\ell^-$ [72].

3.2 Three light mesons

Lattice studies of three-meson systems have been rapidly advancing beyond the first proof-of-concept calculations. Romero-López presented a calculation of the maximal-isospin systems $\pi^+\pi^+\pi^+$, $\pi^+\pi^+K^+$, $\pi^+K^+K^+$, and $K^+K^+K^+$ extending down to the physical pion mass, with the case of pions showing agreement with chiral perturbation theory [73–75]. Other collaborations have investigated three pions with isospin zero [76], one [77], and two [78, 79], which are challenging in part because of ρ and σ resonances appearing in two-particle subsystems. Mai presented the isospin-one study [80], which identified the $J^{PC} = 0^{-+} \pi(1300)$ resonance at pion mass 305 MeV and extrapolated it to the physical pion mass. For lighter pion masses, this would lie above the $5m_\pi$ threshold where the three-particle quantization condition breaks down. For a more detailed discussion of three-particle scattering, see the review talk by Sharpe [48].

3.3 Charmed mesons

Figure 4 shows the experimentally observed low-lying charm-antilight and charm-antistrange mesons. For $J^P = 0^-, 1^-,$ and 2^+ , the typical pattern can be seen: substituting a strange instead of a light antiquark increases the mass by about 100 MeV. One can also identify a pair of 1^+ states that follow the same pattern. However, two strange mesons have unusually low masses compared with the corresponding light meson: $D_{s0}^*(2317)$ and $D_{s1}(2460)$. According to studies in unitarized chiral perturbation theory (UChPT), the resolution of this puzzle is that two of the light mesons, $D_0^*(2300)$ and $D_1(2430)$, have been misidentified and each of them is actually a pair of two distinct poles [81]. In the SU(3) flavour limit, scattering of a $D_{(s)}$ meson and an octet meson belongs to the irreps $\bar{\mathbf{3}} \otimes \mathbf{8} = \bar{\mathbf{3}} \oplus \mathbf{6} \oplus \bar{\mathbf{15}}$; one member of each of these pairs belongs to the conventional $\bar{\mathbf{3}}$ representation and the other belongs to the exotic $\mathbf{6}$ representation containing at least four quarks. The latter also contains manifestly tetraquark states: an $I = 1 T_{c\bar{s}}$ (with some recent evidence for it at LHCb [82]) and an $I = 0 T_{cs}$ with minimal quark content $cs\bar{u}\bar{d}$. UChPT does not predict states in the third representation, $\bar{\mathbf{15}}$, in contrast to diquark-antidiquark models [83]. The ability of lattice

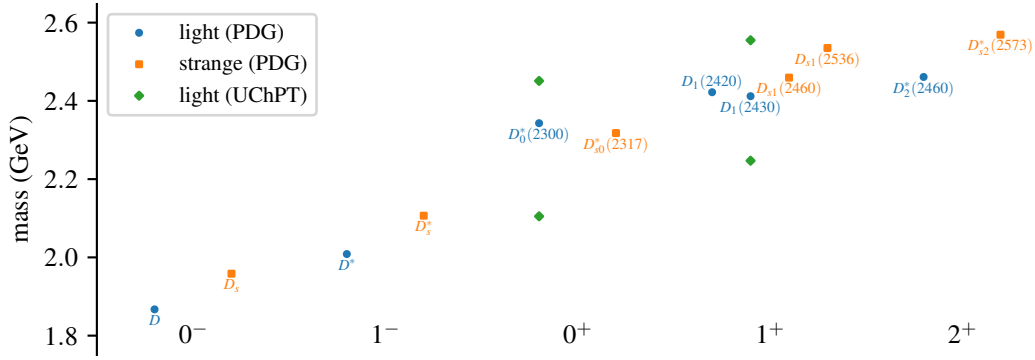


Figure 4: Low-lying D and D_s mesons for various J^P . Blue circles and orange squares indicate light and strange states listed in the PDG [84]; green diamonds show the two-pole structures in the UChPT analysis of Ref. [81].

calculations to vary quark masses and study both SU(3)-symmetric points and the breaking of SU(3) symmetry is thus a great asset for disentangling these models and effective theories.

We first discuss $J^P = 0^+$. In Ref. [85], calculations were done on three volumes at a heavy SU(3) point with $m_\pi = m_K \approx 700$ MeV. In flavour $\bar{\mathbf{3}}$, they found a bound state, in $\mathbf{6}$, they found a virtual state, and in $\bar{\mathbf{15}}$, the behaviour was repulsive. This is consistent with the UChPT prediction. Using previous calculations [86–88], one can track some elements of these multiplets as the pion mass is decreased to 391 and 239 MeV and SU(3) is broken. In the $\bar{\mathbf{3}}$, the D_0^* becomes a resonance, whereas the D_{s0}^* remains a bound state. (A bound D_{s0}^* was previously found in Refs. [89–92].) In the $\mathbf{6}$, only the T_{cs} was studied and was found to remain a virtual state. Other recent studies of S -wave $D\pi$ scattering are Ref. [93], which reaches down to the physical pion mass, and the poster presented by Thoma [94]. Different models for tetraquark states can also be probed via more significant departures from QCD. In Ref. [95], simulations were done with $N_c \in \{3, 4, 5, 6\}$ and SU(4) flavour symmetry; virtual T_{cs} and $T_{c\bar{s}}$ states were only found for $N_c = 3$, which disfavors a compact tetraquark structure.

For $J^P = 1^+$, Ref. [96] worked with broken SU(3) symmetry and studied the coupled-channel system $D^*\pi - D^*\eta - D_s^*\bar{K}$. Consistent with the UChPT picture, three 1^+ states were found: a bound state, a narrow resonance, and a broad resonance. The only calculation with SU(3) symmetry was presented by Gregory [97, 98]. Although it did not include a full scattering analysis, it found that for both $J^P = 0^+$ and 1^+ , the $\mathbf{6}$ was attractive and the $\bar{\mathbf{15}}$ was repulsive, again favouring the molecular picture of UChPT over a compact tetraquark structure.

3.4 Doubly charmed tetraquark

The $T_{cc}(3875)^+$ tetraquark has been of particular interest since its discovery in the $D^0 D^0 \pi^+$ invariant mass spectrum at LHCb [99, 100]. With minimal quark content $cc\bar{u}\bar{d}$ and quantum numbers $I = 0$, $J^P = 1^+$, it lies $360 \pm 40_{-0}^{+4}$ keV below the $D^{*+} D^0$ threshold with a width of $48 \pm 2_{-14}^{+0}$ keV, making it the longest-lived exotic hadron. For pion masses slightly above physical, the D^* becomes stable and we can investigate the T_{cc} as a possible two-body DD^* bound state in the S wave.

An initial group of lattice calculations [101–105], done at pion masses between 146 and 411 MeV for which the D^* is stable, found a virtual state that they identified as the T_{cc} . For decreasing

pion mass, the pole moved toward the DD^* threshold where it would become a bound state. In a coupled-channel analysis, Ref. [105] also found a resonance with strong coupling to D^*D^* .

More recently, there have been more investigations of some sources of systematic uncertainty. Concerning interpolating operators: most spectroscopy calculations used only bilocal operators that resemble noninteracting scattering states, of the form $D(\mathbf{p}_1)D^*(\mathbf{p}_2)$ and $D^*(\mathbf{p}_1)D^*(\mathbf{p}_2)$. However, Ref. [106] found that it is important to also include local four-quark operators (i.e. with smeared $cc\bar{u}\bar{d}$ at the same point) and that without such operators, estimates of some energy levels shift significantly. Stump presented an independent study that confirmed this finding and also showed that including local operators makes the plateau energy estimates much more stable with respect to how many bilocal operators are used [15, 16].

As discussed in Section 2.3, the DD^* partial wave amplitudes have a left-hand cut close to threshold due to u -channel pion exchange. This was neglected in the earlier calculations, which used generalized Lüscher quantization conditions even on this cut where they are invalid. In a reanalysis of the spectrum from Ref. [102] using the plane-wave approach, Ref. [53] found that the T_{cc} was a subthreshold resonance rather than a virtual state. Applying the three-particle approach to the same dataset led to the same conclusion [58]. Raposo presented a new calculation with pion mass 280 MeV and a preliminary analysis using the three-body approach [59], including lattice data for the relevant two-body subchannels, $I = 1 DD$ and $I = 1/2 D\pi$. This method is particularly suited for the T_{cc} as the pion mass is decreased toward its physical value, because it is also valid above the $DD\pi$ threshold. On the other hand, because it treats the D^* as a two-body $D\pi$ bound state, going above the D^*D^* threshold would require a not-yet-available four-particle formalism. The preferred quantization condition thus depends on the physics of interest: at heavier pion masses, two-body methods that include coupled channels and left-hand cuts can be used to analyze energy levels above the D^*D^* threshold, whereas at light pion masses the three-body method is best for the T_{cc} .

There have been several additional studies of the T_{cc} and related doubly charmed systems such as $I = 1$ and the singly strange $DD_s^*-D^*D_s$ coupled-channel system, which have not found additional tetraquark states [54, 107–111]. This includes talks by Padmanath [112], Shrimal [55], and Mohanta [113].

3.5 Doubly bottom tetraquark

By replacing the two charm quarks in the T_{cc} with bottom quarks, we obtain a conjectured state typically called T_{bb} that couples to $\bar{B}\bar{B}^*$. Several independent lattice calculations using different methods predict a deeply bound state with binding energy of order 100 MeV, as shown in Fig. 5 which includes the study presented by Tripathy [128]. At the physical pion mass, the left-hand cut due to pion exchange starts just 1 MeV below threshold, which makes an analysis of this state using Lüscher's finite-volume quantization condition invalid [117]. However, since this state is deeply bound, we expect exponentially suppressed finite-volume effects.

This doubly bottom tetraquark is a good opportunity for lattice QCD calculations to make a precise prediction ahead of a possible future experimental discovery. It is therefore important to carefully examine possible sources of systematic uncertainty. One reason for concern is the use of asymmetric correlation functions (typically with wall sources) in some of these calculations. Ref. [117] is particularly important for having addressed this by employing a symmetric correlator matrix with both local and bilocal interpolating operators. They found that the bilocal operators had

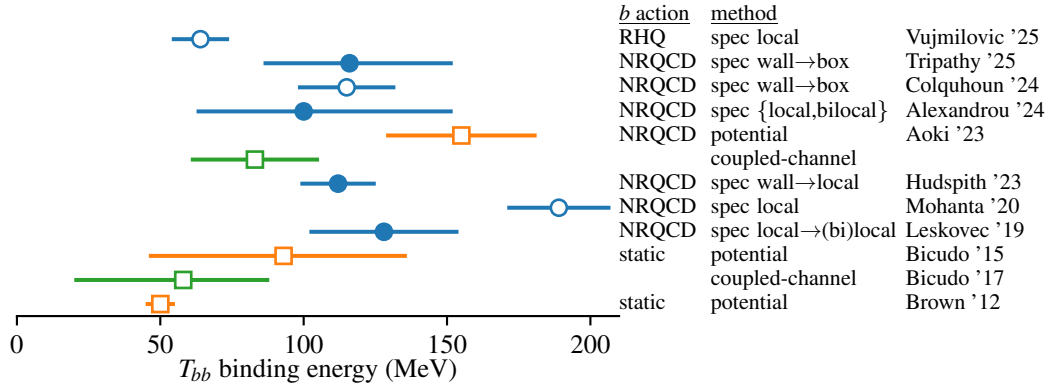


Figure 5: Lattice calculations of the T_{bb} binding energy, determined using finite-volume spectroscopy [114–120] (blue circles) and potentials via the Born-Oppenheimer [121–123] and HAL QCD [124] methods (orange squares for single channel and green squares for coupled channel). Open symbols indicate a single lattice spacing or a single pion mass was used. Some earlier calculations that have been superseded [125–127] are omitted from this figure.

no effect on the estimate of the ground-state energy, which helps to support the findings of previous calculations. On the other hand, it was recently shown that using only bilocal operators without local operators yields a poor estimate of the ground-state energy [106].

Being a stable hadron makes studying the structure of the T_{bb} much simpler than for exotic resonances. Vujmilovic presented a calculation of its electromagnetic form factors [120, 129]. It was found that the charge radius of the T_{bb} is smaller than for a B or B^* meson and that the magnetic moment is almost entirely produced by the b quarks; this was interpreted as favouring a structure in which a bb 1^+ diquark is bound in S -wave with a $\bar{u}\bar{d}$ 0^+ antiquark.

3.6 Other heavy hadrons

For hadrons containing any combination of light quarks and gluons plus either two heavy quarks or a heavy quark-antiquark pair, the Born-Oppenheimer approach is an alternative to the Lüscher method: one computes potentials for a pair of static (anti)quarks plus the dynamical light degrees of freedom, then solves a Schrödinger equation for the heavy quarks. Mohapatra presented a Born-Oppenheimer EFT for exotic hadrons including the T_{cc} and T_{bb} [130–133], whereas calculations of the potentials were presented in the talk by Sharma [134] and the poster by Picão [135].

A few talks covered studies of charmonium. Bali presented a calculation of η_c and J/ψ masses on about 50 ensembles from CLS, with the usual approximation of no $c\bar{c}$ annihilation [136]. In contrast, Urrea-Niño showed the effect of removing this approximation on one ensemble with dynamical charm quarks [11, 137].

Stable baryons containing charm and/or bottom quarks, many of which have not yet been discovered experimentally, were presented in three talks, all using HISQ ensembles. Shaikh employed a mixed action setup with NRQCD bottom action, RHQ charm action, and clover light-quark action [138], whereas Radhakrishnan used HISQ for all flavours and a very fine lattice [139]. Dhindsa presented a precise study of two Ω_{ccc} baryons using both overlap and HISQ actions for the valence charm quarks [140, 141].

3.7 Systems with baryons

The only talk about stable light baryons was by Rosso, who focussed on the complications arising from C -periodic boundary conditions [142]. Precision calculations of the Ω mass have played an important role in scale setting, particularly for the muon $g - 2$ [143, 144]. In order to establish strong control over excited-state contributions in these high-precision calculations, perhaps it may be useful to employ techniques used for multiparticle spectroscopy.

In the baryon-meson sector, there are an increasing number of studies of $N\pi$ physics, even to the point of explicitly controlling intermediate $N\pi$ states in a study of nucleon polarizabilities and calculating $\gamma^*N \rightarrow \pi N$ multipole amplitudes [145, 146]. Paul presented an ongoing study of $N \rightarrow \Delta(1232)$ resonance transition form factors, which require analytically continuing $N \rightarrow N\pi$ transition amplitudes to the resonance pole [147].

There has been some interest in the $J^P = \frac{1}{2}^-$ $\Lambda(1405)$ resonance, because it has also been suggested to have a two-pole structure (similar to the D mesons discussed in Section 3.3) with one belonging to the SU(3) octet and the other to the singlet [now listed as the two-star $\Lambda(1380)$ in the PDG]. A first study of $\pi\Sigma-\bar{K}N$ coupled channels indeed found both a virtual state and a resonance at pion mass 200 MeV [148, 149]. Mai presented a combined analysis of those lattice data and experiment using UChPT [150, 151], whereas an extension of that project to different pion masses and other negative-parity hyperons was presented by Alvarado [152]. Finally, a study with SU(3) symmetry and pion mass 700 MeV was presented by Sucunza [153].

Two studies of baryon-meson scattering at the physical pion mass and investigations of possible pentaquarks using the HAL QCD method were reported: KN by Murakami [154, 155] and $\bar{D}N$ by Yamada [156, 157].

Concerning baryon-baryon calculations, I refer to Nicholson's plenary talk for the current status of NN [30]. Other talks on NN were given by Perry [43], Chakraborty [23], and Sugiura [13]. Channels involving hyperons were discussed by Laudicina [158] and Murase [159].

4. Outlook

The field of two-hadron spectroscopy using lattice QCD is maturing. Many hadronic systems of interest have been studied by multiple independent collaborations. Still, there are some new methodological developments such as the treatment of left-hand cuts in finite-volume quantization conditions.

A better understanding of systematic errors is needed. This includes errors associated with the choice of interpolating operators, plateau fits or other methods for estimating energy levels, and the modelling of scattering amplitudes. More investigation of standard lattice artifacts such as discretization effects would also be valuable: it was found that the latter can be quite significant in baryon-baryon systems [24, 29, 160]. Obtaining full control over uncertainties is essential for making precise QCD predictions and making the connection with experiment.

For many hadrons, an obstacle to decreasing the pion mass towards its physical value is the opening of new channels with three or more hadrons. The necessary three-hadron spectroscopy is a relatively new field that has made significant progress in recent years but with much pioneering work still to come.

Acknowledgments

I thank everyone who communicated with me about their results: J. Baeza Ballesteros, D. Chakraborty, X. Feng, M. Mai, N. Mathur, K. Murakami, M. Padmanath, R. Perry, A. Portelli, S. Prelovšek, J. T. Tsang, F. Romero-López, M. Salg, T. Scirpa, J. A. Urrea-Niño, and I. Vujmilovic.

The correlation functions used to produce Fig. 2 were computed using resources provided by the Gauss Centre for Supercomputing e.V. (www.gauss-centre.eu) on JUWELS [161] at Jülich Supercomputing Centre. This work used the software packages QDP++ [162], PRIMME [163], QUDA [164–167], NumPy [168], SciPy [169], CuPy [170], and Matplotlib [171].

References

- [1] L. Barca, *Evidence of current-enhanced excited states in lattice QCD three-point functions*, *PoS LATTICE2025* 004 [2602.17195].
- [2] C. Alexandrou, L. Leskovec, S. Meinel et al., *Phys. Rev. D* **96** (2017) 034525 [1704.05439].
- [3] G. Silvi et al., *Phys. Rev. D* **103** (2021) 094508 [2101.00689].
- [4] L. Barca, G. Bali and S. Collins, *Phys. Rev. D* **107** (2023) L051505 [2211.12278].
- [5] W. Detmold, D.J. Murphy et al., *Phys. Rev. D* **104** (2021) 034502 [1908.07050].
- [6] Y. Li, S.-C. Xia, X. Feng et al., *Phys. Rev. D* **103** (2021) 014514 [2009.01029].
- [7] HADRON SPECTRUM collaboration, *Phys. Rev. D* **80** (2009) 054506 [0905.2160].
- [8] C. Morningstar, J. Bulava, J. Foley et al., *Phys. Rev. D* **83** (2011) 114505 [1104.3870].
- [9] F. Knechtli, T. Korzec et al., *Phys. Rev. D* **106** (2022) 034501 [2205.11564].
- [10] J.A. Urrea-Niño, F. Knechtli, T. Korzec and M. Peardon, 2603.20178.
- [11] J.A. Urrea-Niño, *Mixing of light meson and charmonium flavor singlets in $N_f = 3 + 1$ QCD*, *PoS LATTICE2025* 079.
- [12] T. Sugiura, Y. Akahoshi, T. Aoyama et al., *PoS LATTICE2021* (2022) 565 [2202.12532].
- [13] T. Sugiura, *Quark mass dependence of the nuclear LS force*, *PoS LATTICE2025* 060.
- [14] HADRON SPECTRUM collaboration, *Phys. Rev. D* **111** (2025) 114510 [2411.10395].
- [15] A. Stump and J.R. Green, *Phys. Rev. D* **113** (2026) 034513 [2510.26459].
- [16] A. Stump and J.R. Green, *Importance of local tetraquark operators for $T_{cc}(3875)^+$* , *PoS LATTICE2025* 062 [2602.20848].
- [17] T. Doi and M.G. Endres, *Comput. Phys. Commun.* **184** (2013) 117 [1205.0585].
- [18] W. Detmold and K. Orginos, *Phys. Rev. D* **87** (2013) 114512 [1207.1452].

- [19] B. Hörz and A. Hanlon, *Phys. Rev. Lett.* **123** (2019) 142002 [1905.04277].
- [20] J. Chen, R.G. Edwards and W. Mao, *Graph contractions for calculating correlation functions in lattice QCD*, in *Platform for Advanced Scientific Computing*, 2023, DOI.
- [21] D. Chakraborty, P. Srivastava et al., *Phys. Rev. D* **110** (2024) 114505 [2411.08962].
- [22] O. Selvitopi, E. Ozturk, J. Chen, P. Sadayappan, R.G. Edwards and A. Buluç, 2511.02257.
- [23] D. Chakraborty, *Investigating quark mass dependence of nuclear binding from lattice QCD*, *PoS LATTICE2025* 071.
- [24] J.R. Green, A.D. Hanlon et al., *Phys. Rev. Lett.* **127** (2021) 242003 [2103.01054].
- [25] C. Michael, *Nucl. Phys. B* **259** (1985) 58.
- [26] M. Lüscher and U. Wolff, *Nucl. Phys. B* **339** (1990) 222.
- [27] B. Blossier, M. Della Morte, G. von Hippel et al., *JHEP* **04** (2009) 094 [0902.1265].
- [28] T. Iritani et al., *JHEP* **10** (2016) 101 [1607.06371].
- [29] J.R. Green, *PoS CD2024* (2026) 019 [2502.15546].
- [30] A. Nicholson, *NN scattering: past, present, and future*, *PoS LATTICE2025* 006.
- [31] BARYON SCATTERING collaboration, *Phys. Rev. C* **113** (2026) 024002 [2505.05547].
- [32] A. Portelli and J.T. Tsang, *Phys. Rev. D* **112** (2025) 094512 [2508.11541].
- [33] M.L. Wagman, *Phys. Rev. Lett.* **134** (2025) 241901 [2406.20009].
- [34] D.C. Hackett and M.L. Wagman, *Phys. Rev. D* **112** (2025) 014514 [2412.04444].
- [35] J. Ostmeyer, A. Sen and C. Urbach, *Eur. Phys. J. A* **61** (2025) 26 [2411.14981].
- [36] D. Chakraborty, D. Sood et al., *Phys. Rev. D* **112** (2025) 074506 [2412.01900].
- [37] R. Abbott, D.C. Hackett, G.T. Fleming, D.A. Pefkou and M.L. Wagman, 2503.17357.
- [38] J. Ostmeyer and C. Urbach, 2510.15500.
- [39] R. Tsuji, S. Hashimoto and R. Kellermann, 2511.05058.
- [40] J. Ostmeyer, *The truncated Hankel correlator (THC) method*, *PoS LATTICE2025* 039.
- [41] NPLQCD collaboration, 2601.22273.
- [42] NPLQCD collaboration, 2601.22272.
- [43] R. Perry, *Systematic uncertainties in two-nucleon spectroscopy*, *PoS LATTICE2025* 058.
- [44] J. Moscoso, F.G. Ortega-Gama, R.A. Briceño, A.W. Jackura et al., 2602.20373.

- [45] F.G. Ortega-Gama, *Two-particle matrix elements in a box*, *PoS LATTICE2025* 068.
- [46] M.T. Hansen, F. Romero-López and S.R. Sharpe, *JHEP* **02** (2026) 221 [2509.24778].
- [47] S.R. Sharpe, *Extending the finite volume formalism to the $N\pi\pi$ system at maximal isospin*, *PoS LATTICE2025* 073.
- [48] S.R. Sharpe, *Three-particle scattering amplitudes from lattice QCD*, *PoS LATTICE2025* 021 [2601.04147].
- [49] R. Mukherjee, *Towards four-pion effects in multi-hadron decays*, *PoS LATTICE2025* 090.
- [50] M.-L. Du, A. Filin, V. Baru et al., *Phys. Rev. Lett.* **131** (2023) 131903 [2303.09441].
- [51] A.B. Raposo and M.T. Hansen, *JHEP* **08** (2024) 075 [2311.18793].
- [52] L. Meng and E. Epelbaum, *JHEP* **10** (2021) 051 [2108.02709].
- [53] L. Meng, V. Baru, E. Epelbaum et al., *Phys. Rev. D* **109** (2024) L071506 [2312.01930].
- [54] T. Shrimal, S. Collins, P. Jana et al., *Phys. Rev. D* **112** (2025) 054513 [2504.16931].
- [55] T. Shrimal, S. Collins, P. Jana, M. Padmanath and S. Prelovsek, *Strange partner of T_{cc}^+ from lattice QCD in $D^{(*)}D_s^{(*)}$ scattering*, *PoS LATTICE2025* 061 [2603.19784].
- [56] A.B. Raposo, R.A. Briceño et al., *JHEP* **06** (2025) 186 [2502.19375].
- [57] M.T. Hansen, F. Romero-López and S.R. Sharpe, *JHEP* **06** (2024) 051 [2401.06609].
- [58] S.M. Dawid, F. Romero-López and S.R. Sharpe, *JHEP* **01** (2025) 060 [2409.17059].
- [59] H. Alharazin, A.B. Raposo, J. Bulava, S. Dawid, J.R. Green et al., *Three-body study of the $T_{cc}(3875)^+$ from lattice QCD*, *PoS LATTICE2025* 085 [2602.17204].
- [60] R. Bubna, H.-W. Hammer, F. Müller, J.-Y. Pang et al., *JHEP* **05** (2024) 168 [2402.12985].
- [61] R. Bubna, H.-W. Hammer, B.-L. Hoid, J.-Y. Pang et al., *JHEP* **10** (2025) 197 [2507.18399].
- [62] S.M. Dawid et al., *Phys. Lett. B* **864** (2025) 139442 [2411.15730].
- [63] HADRON SPECTRUM collaboration, *Phys. Rev. D* **109** (2024) 034513 [2304.03762].
- [64] M. Salg, F. Romero-López and W.I. Jay, *Phys. Rev. D* **112** (2025) 114502 [2506.16161].
- [65] M. Salg, *Bayesian analysis and analytic continuation of scattering amplitudes from lattice QCD*, *PoS LATTICE2025* 078.
- [66] P. Boyle, F. Erben, V. Gülpers et al., *Phys. Rev. Lett.* **134** (2025) 111901 [2406.19194].
- [67] P. Boyle, F. Erben, V. Gülpers et al., *Phys. Rev. D* **111** (2025) 054510 [2406.19193].
- [68] EXTENDED TWISTED MASS, ETM collaboration, *Phys. Lett. B* **819** (2021) 136449 [2006.13805].

- [69] CLQCD collaboration, *JHEP* **08** (2025) 064 [2502.03700].
- [70] A.D.M. Valois, *$\pi\pi$ scattering from lattice QCD with staggered quarks*, *PoS LATTICE2025* 077.
- [71] G. Morandi, M. Bruno, F.A. Bresciani, C. Lehner and J. Parrino, *Towards the time-like pion form factor beyond the elastic regime using domain-wall QCD*, *PoS LATTICE2025* 083 [2603.04094].
- [72] F. Erben, M. Black, P. Boyle, M. Di Carlo, V. Gülpers, M.T. Hansen et al., *$K\pi$ scattering as a step towards $B \rightarrow K^*\ell^+\ell^-$ from lattice QCD*, *PoS LATTICE2025* 245 [2603.17900].
- [73] S.M. Dawid, Z.T. Draper et al., *Phys. Rev. Lett.* **135** (2025) 021903 [2502.14348].
- [74] S.M. Dawid, Z.T. Draper et al., *Phys. Rev. D* **112** (2025) 014505 [2502.17976].
- [75] F. Romero-López, *QCD predictions for physical multimeson scattering amplitudes*, *PoS LATTICE2025* 089.
- [76] H. Yan, M. Mai, M. Garofalo et al., *Phys. Rev. Lett.* **133** (2024) 211906 [2407.16659].
- [77] H. Yan, M. Mai, M. Garofalo, Y. Feng, M. Döring, C. Liu et al., 2510.09476.
- [78] R.A. Briceño, M.T. Hansen, A.W. Jackura, R.G. Edwards and C.E. Thomas, 2510.24894.
- [79] Y. Feng, C. Culver, M. Döring, M. Mai, A. Alexandru and F.X. Lee, 2601.16916.
- [80] M. Mai, *Emergence of the $\pi(1300)$ -resonance from lattice QCD*, *PoS LATTICE2025* 091.
- [81] M.-L. Du, M. Albaladejo et al., *Phys. Rev. D* **98** (2018) 094018 [1712.07957].
- [82] LHCb collaboration, *Sci. Bull.* **70** (2025) 1432 [2411.03399].
- [83] F.-K. Guo and B.-S. Zou, *Sci. Bull.* **70** (2025) 2535 [2504.21442].
- [84] PARTICLE DATA GROUP collaboration, *Phys. Rev. D* **110** (2024) 030001.
- [85] HADRON SPECTRUM collaboration, *JHEP* **07** (2024) 012 [2403.10498].
- [86] G. Moir, M. Peardon, S.M. Ryan et al., *JHEP* **10** (2016) 011 [1607.07093].
- [87] HADRON SPECTRUM collaboration, *JHEP* **02** (2021) 100 [2008.06432].
- [88] HADRON SPECTRUM collaboration, *JHEP* **07** (2021) 123 [2102.04973].
- [89] D. Mohler, C.B. Lang, L. Leskovec et al., *Phys. Rev. Lett.* **111** (2013) 222001 [1308.3175].
- [90] C.B. Lang, L. Leskovec, D. Mohler et al., *Phys. Rev. D* **90** (2014) 034510 [1403.8103].
- [91] G.S. Bali, S. Collins, A. Cox and A. Schäfer, *Phys. Rev. D* **96** (2017) 074501 [1706.01247].
- [92] C. Alexandrou, J. Berlin, J. Finkenrath et al., *Phys. Rev. D* **101** (2020) 034502 [1911.08435].

- [93] H. Yan, C. Liu, L. Liu et al., *Phys. Rev. D* **111** (2025) 014503 [2404.13479].
- [94] D. Thoma, *Investigations of a novel fully relativistic heavy-quark action in D meson systems*, *PoS LATTICE2025* 260.
- [95] J. Baeza-Ballesteros et al., *JHEP* **08** (2025) 110 [2503.13978].
- [96] HADRON SPECTRUM collaboration, *JHEP* **07** (2025) 060 [2502.04232].
- [97] E.B. Gregory, F.-K. Guo, C. Hanhart, S. Krieg and T. Luu, *Eur. Phys. J. A* **61** (2025) 226 [2503.23954].
- [98] E.B. Gregory, *The structure of the lightest positive-parity charmed mesons from LQCD*, *PoS LATTICE2025* 082.
- [99] LHC_B collaboration, *Nature Phys.* **18** (2022) 751 [2109.01038].
- [100] LHC_B collaboration, *Nature Commun.* **13** (2022) 3351 [2109.01056].
- [101] Y. Ikeda, B. Charron, S. Aoki, T. Doi, T. Hatsuda, T. Inoue et al., *Phys. Lett. B* **729** (2014) 85 [1311.6214].
- [102] M. Padmanath and S. Prelovsek, *Phys. Rev. Lett.* **129** (2022) 032002 [2202.10110].
- [103] S. Chen, C. Shi, Y. Chen, M. Gong, Z. Liu, W. Sun et al., *Phys. Lett. B* **833** (2022) 137391 [2206.06185].
- [104] Y. Lyu, S. Aoki, T. Doi, T. Hatsuda, Y. Ikeda and J. Meng, *Phys. Rev. Lett.* **131** (2023) 161901 [2302.04505].
- [105] HADRON SPECTRUM collaboration, *Phys. Rev. D* **111** (2025) 034511 [2405.15741].
- [106] S. Prelovsek, E. Ortiz-Pacheco, S. Collins, L. Leskovec, M. Padmanath and I. Vujmilovic, *Phys. Rev. D* **112** (2025) 014507 [2504.03473].
- [107] S. Collins, A. Nefediev, M. Padmanath and S. Prelovsek, *Phys. Rev. D* **109** (2024) 094509 [2402.14715].
- [108] L. Meng, E. Ortiz-Pacheco, V. Baru, E. Epelbaum, M. Padmanath and S. Prelovsek, *Phys. Rev. D* **111** (2025) 034509 [2411.06266].
- [109] P.-P. Shi, F.-K. Guo, C. Liu, L. Liu, P. Sun, J.-J. Wu et al., 2502.07438.
- [110] HADRON SPECTRUM collaboration, *Phys. Rev. D* **112** (2025) 114511 [2505.01363].
- [111] M. Nagatsuka and S. Sasaki, *Phys. Rev. D* **112** (2025) 114510 [2507.20712].
- [112] M. Padmanath, *Charm tetraquarks investigation using CLS lattices*, *PoS LATTICE2025* 059.
- [113] P. Mohanta, S. Paul and S. Basak, *T_{cc} pole trajectory*, *PoS LATTICE2025* 066 [2603.01259].

- [114] L. Leskovec, S. Meinel, M. Pflaumer and M. Wagner, *Phys. Rev. D* **100** (2019) 014503 [1904.04197].
- [115] P. Mohanta and S. Basak, *Phys. Rev. D* **102** (2020) 094516 [2008.11146].
- [116] R.J. Hudspith and D. Mohler, *Phys. Rev. D* **107** (2023) 114510 [2303.17295].
- [117] C. Alexandrou, J. Finkenrath, T. Leontiou, S. Meinel, M. Pflaumer and M. Wagner, *Phys. Rev. D* **110** (2024) 054510 [2404.03588].
- [118] B. Colquhoun, A. Francis, R.J. Hudspith, R. Lewis, K. Maltman and W.G. Parrott, *Phys. Rev. D* **110** (2024) 094503 [2407.08816].
- [119] B.S. Tripathy, N. Mathur and M. Padmanath, *Phys. Rev. D* **111** (2025) 114504 [2503.09760].
- [120] I. Vujmilovic, S. Collins, L. Leskovec and S. Prelovsek, 2510.17549.
- [121] Z.S. Brown and K. Orginos, *Phys. Rev. D* **86** (2012) 114506 [1210.1953].
- [122] P. Bicudo, K. Cichy, A. Peters, B. Wagenbach and M. Wagner, *Phys. Rev. D* **92** (2015) 014507 [1505.00613].
- [123] P. Bicudo, J. Scheunert and M. Wagner, *Phys. Rev. D* **95** (2017) 034502 [1612.02758].
- [124] T. Aoki, S. Aoki and T. Inoue, *Phys. Rev. D* **108** (2023) 054502 [2306.03565].
- [125] EUROPEAN TWISTED MASS collaboration, *Phys. Rev. D* **87** (2013) 114511 [1209.6274].
- [126] A. Francis, R.J. Hudspith, R. Lewis and K. Maltman, *Phys. Rev. Lett.* **118** (2017) 142001 [1607.05214].
- [127] P. Junnarkar, N. Mathur and M. Padmanath, *Phys. Rev. D* **99** (2019) 034507 [1810.12285].
- [128] B.S. Tripathy, N. Mathur and M. Padmanath, *Doubly bottom and bottom-strange tetraquarks in the isoscalar channel*, *PoS LATTICE2025* 063 [2603.18667].
- [129] I. Vujmilovic, S. Collins, L. Leskovec and S. Prelovsek, *Electromagnetic form factors and structure of the T_{bb} tetraquark*, *PoS LATTICE2025* 076 [2602.24000].
- [130] M. Berwein, N. Brambilla, A. Mohapatra and A. Vairo, *Phys. Rev. D* **110** (2024) 094040 [2408.04719].
- [131] N. Brambilla, A. Mohapatra, T. Scirpa and A. Vairo, *Phys. Rev. Lett.* **135** (2025) 131902 [2411.14306].
- [132] N. Brambilla, A. Mohapatra and A. Vairo, *Phys. Rev. D* **112** (2025) 114037 [2508.13050].
- [133] A. Mohapatra, *Born-Oppenheimer effective theory for multi-quark states*, *PoS LATTICE2025* 064.

- [134] S. Sharma, *Adjoint meson and tetraquark static energies using novel BOEFT interpolators*, *PoS LATTICE2025* 086.
- [135] B.M.C.R.C. Picão, *$\bar{Q}\bar{Q}qq$ potentials and disentanglement of excited states*, *PoS LATTICE2025* 261.
- [136] G. Bali, *Precision charmonium spectroscopy on CLS ensembles: an update*, *PoS LATTICE2025* 074.
- [137] J.A. Urrea-Niño, R. Höllwieser, F. Knechtli, T. Korzec, J. Finkenrath and M. Peardon, *Phys. Rev. D* **112** (2025) 074502 [2506.22132].
- [138] S. Shaikh, P. Mohanta, M. Padmanath and S. Basak, *Heavy hadron spectrum from 2+1+1 flavor MILC lattices*, *PoS LATTICE2025* 081 [2601.07360].
- [139] A. Radhakrishnan, *Studying heavy hadrons with relativistic quarks*, *PoS LATTICE2025* 072.
- [140] N.S. Dhindsa, D. Chakraborty, A. Radhakrishnan, N. Mathur and M. Padmanath, *Phys. Rev. D* **112** (2025) L111501 [2411.12729].
- [141] N.S. Dhindsa, D. Chakraborty et al., *Precisely determining the ground state mass of spin-3/2 Ω_{ccc} baryon from lattice QCD*, *PoS LATTICE2025* 069 [2512.23417].
- [142] A. Altherr, I. Campos, R. Gruber, T. Harris, F. Margari, M. Krstić Marinković et al., *Baryon masses with C-periodic boundary conditions*, *PoS LATTICE2025* 080 [2602.23910].
- [143] A. Boccaletti et al., 2407.10913.
- [144] FERMILAB LATTICE, MILC collaboration, *Phys. Rev. D* **113** (2026) 054501 [2509.14367].
- [145] X.-H. Wang, Z.-L. Zhang, X.-H. Cao, C.-L. Fan, X. Feng, Y.-S. Gao et al., *Phys. Rev. Lett.* **133** (2024) 141901 [2310.01168].
- [146] Y.-S. Gao, Z.-L. Zhang, X. Feng, L.-C. Jin, C. Liu and U.-G. Meißner, *Phys. Rev. Lett.* **134** (2025) 171904 [2502.12074].
- [147] S. Paul, *$N \rightarrow \Delta(1232)$ resonance transition form factors from lattice QCD*, *PoS LATTICE2025* 067.
- [148] BARYON SCATTERING (BASc) collaboration, *Phys. Rev. Lett.* **132** (2024) 051901 [2307.10413].
- [149] BARYON SCATTERING (BASc) collaboration, *Phys. Rev. D* **109** (2024) 014511 [2307.13471].
- [150] F. Pittler, M. Mai, U.-G. Meißner, R.F. Ferguson, P. Hurck, D.G. Ireland et al., *Phys. Rev. D* **112** (2025) 074037 [2507.14283].
- [151] M. Mai, *A curious case of a strangeness resonance — lattice and experiment*, *PoS LATTICE2025* 065.

- [152] F. Alvarado, *Negative parity hyperons from coupled channel scattering*, *PoS LATTICE2025* 088.
- [153] J.S. Sucunza, T. Luu and C. Urbach, *The Lambda 1405 at the SU(3) point in lattice QCD*, *PoS LATTICE2025* 092 [2602.19928].
- [154] HAL QCD collaboration, *Phys. Rev. D* **113** (2026) 054506 [2509.00838].
- [155] K. Murakami, *Lattice QCD study on kaon-nucleon interactions and Θ^+ pentaquark on the physical point*, *PoS LATTICE2025* 087.
- [156] W. Yamada, Y. Lyu, K. Murakami and T. Doi, 2603.12251.
- [157] W. Yamada, *$\bar{D}N$ interaction from lattice QCD at the physical point*, *PoS LATTICE2025* 084.
- [158] BAsC collaboration, *Preliminary study of the H dibaryon in $N_f = 2 + 1$ lattice QCD*, *PoS LATTICE2025* 075 [2603.00698].
- [159] K. Murase, *Physical-point lattice QCD study of baryon-baryon interactions in the $S = -1$ channel*, *PoS LATTICE2025* 070.
- [160] HAL QCD collaboration, *Few Body Syst.* **65** (2024) 34.
- [161] Jülich Supercomputing Centre, *J. Large-Scale Res. Facil.* **7** (2021) A183.
- [162] SciDAC, LHPC, UKQCD collaboration, *Nucl. Phys. B (Proc. Suppl.)* **140** (2005) 832 [hep-lat/0409003].
- [163] A. Stathopoulos and J.R. McCombs, *ACM Trans. Math. Softw.* **37** (2010) 21:1.
- [164] QUDA collaboration, *Comput. Phys. Commun.* **181** (2010) 1517 [0911.3191].
- [165] QUDA collaboration, *Scaling lattice QCD beyond 100 GPUs*, in *SC '11: Proceedings of the International Conference for High Performance Computing, Networking, Storage and Analysis*, 9, 2011 [1109.2935].
- [166] QUDA collaboration, *Accelerating lattice QCD multigrid on GPUs using fine-grained parallelization*, in *SC '16: Proceedings of the International Conference for High Performance Computing, Networking, Storage and Analysis*, 12, 2016 [1612.07873].
- [167] M.A. Clark et al., 2510.26313.
- [168] C.R. Harris, K.J. Millman, S.J. van der Walt et al., *Nature* **585** (2020) 357 [2006.10256].
- [169] P. Virtanen, R. Gommers, T.E. Oliphant et al., *Nature Methods* **17** (2020) 261 [1907.10121].
- [170] R. Okuta, Y. Unno, D. Nishino, S. Hido and C. Loomis, *CuPy: A NumPy-compatible library for NVIDIA GPU calculations*, in *Proceedings of Workshop on Machine Learning Systems (LearningSys) in The Thirty-first Annual Conference on Neural Information Processing Systems (NIPS)*, 2017.
- [171] J.D. Hunter, *Comput. Sci. Eng.* **9** (2007) 90.